Circulation Research

ORIGINAL RESEARCH

AKAP12 Upregulation Associates With PDE8A to Accelerate Cardiac Dysfunction

Hanan Qasim, Mehrdad Rajaei, Ying Xu, Arfaxad Reyes-Alcaraz, Hala Y. Abdelnasser, M. David Stewart, Satadru K. Lahiri, Xander H.T. Wehrens, Bradley K. McConnell

BACKGROUND: In heart failure, signaling downstream the β2-adrenergic receptor is critical. Sympathetic stimulation of β2-adrenergic receptor alters cAMP (cyclic adenosine 3′,5′-monophosphate) and triggers PKA (protein kinase A)-dependent phosphorylation of proteins that regulate cardiac function. cAMP levels are regulated in part by PDEs (phosphodiesterases). Several AKAPs (A kinase anchoring proteins) regulate cardiac function and are proposed as targets for precise pharmacology. AKAP12 is expressed in the heart and has been reported to directly bind β2-adrenergic receptor, PKA, and PDE4D. However, its roles in cardiac function are unclear.

METHODS: cAMP accumulation in real time downstream of the β2-adrenergic receptor was detected for 60 minutes in live cells using the luciferase-based biosensor (GloSensor) in AC16 human-derived cardiomyocyte cell lines overexpressing AKAP12 versus controls. Cardiomyocyte intracellular calcium and contractility were studied in adult primary cardiomyocytes from male and female mice overexpressing cardiac AKAP12 ($AKAP12^{OX}$) and wild-type littermates post acute treatment with 100-nM isoproterenol (ISO). Systolic cardiac function was assessed in mice after 14 days of subcutaneous ISO administration (60 mg/kg per day). AKAP12 gene and protein expression levels were evaluated in left ventricular samples from patients with end-stage heart failure.

RESULTS: AKAP12 upregulation significantly reduced total intracellular cAMP levels in AC16 cells through PDE8. Adult primary cardiomyocytes from $AKAP12^{OX}$ mice had significantly reduced contractility and impaired calcium handling in response to ISO, which was reversed in the presence of the selective PDE8 inhibitor (PF-04957325). $AKAP12^{OX}$ mice had deteriorated systolic cardiac function and enlarged left ventricles. Patients with end-stage heart failure had upregulated gene and protein levels of AKAP12.

CONCLUSIONS: AKAP12 upregulation in cardiac tissue is associated with accelerated cardiac dysfunction through the AKAP12-PDE8 axis.

GRAPHIC ABSTRACT: A graphic abstract is available for this article.

Key Words: A kinase anchor proteins ■ calcium ■ echocardiography ■ heart ■ myocytes, cardiac ■ receptors, adrenergic, beta

Meet the First Author, see p 953 | Editorial, see p 1023

Heart failure (HF) is a chronic disease in which the heart cannot pump enough blood to meet the body's demands.[1] This impaired pumping of blood is partially due to insufficient contraction, which is highly regulated by GPCRs (G-protein coupled receptors); βARs (β-adrenergic receptors).[1] Downstream of βARs, cAMP (cyclic adenosine 3′,5′-monophosphate) is a second messenger that plays a major role in cardiac excitation-contraction coupling (ECC).[2,3] The intracellular levels of cAMP are finely tuned based on the activities of ACs (adenylyl cyclases; enzymes that increase cAMP levels) and PDEs (phosphodiesterases; enzymes that reduce cAMP levels).[1,4] To further ensure a more specific cellular response to distinct stimuli, spatial and temporal localization of cAMP is associated with AKAPs (A kinase anchoring proteins).[5–7]

Correspondence to: Bradley K. McConnell, PhD, Department of Pharmacological and Pharmaceutical Sciences, University of Houston College of Pharmacy, 4349 Martin Luther King Blvd, Health-2 (H2) Bldg, Rm 5024, Houston, TX 77204-5037. Email bkmcconn@central.uh.edu
Supplemental Material is available at https://www.ahajournals.org/doi/suppl/10.1161/CIRCRESAHA.123.323655.
For Sources of Funding and Disclosures, see page 1020–1021.

Circulation Research is available at www.ahajournals.org/journal/res

Novelty and Significance

What Is Known?

- AKAPs (A kinase anchoring proteins) form signalosomes that regulate cardiac function.
- AKAP12 scaffolds PKA (protein kinase A), and β-adrenergic receptor, both of which are important for cardiac contractility.
- Cardiac AKAP12's roles are unclear.

What New Information Does This Article Contribute?

- PDE8A (phosphodiesterase 8A) is in the vicinity of the AKAP12 signalosome.
- Specific AKAP12 upregulation in mouse cardiomyocytes significantly reduces cardiomyocyte contractility, which is reversed by inhibiting PDE8.
- AKAP12 upregulation in cardiac tissue accelerates cardiac maladaptive remodeling in animal models, and patients with end-stage heart failure have upregulated gene and protein levels of AKAP12.

This article delves into the intricate signaling mechanisms of cardiac function, focusing on the role of AKAPs, specifically AKAP12. While AKAPs are known to form essential microdomains within cells, regulating cardiac function by scaffolding proteins like PKA and β-adrenergic receptor, the specific functions of AKAP12 in the heart remained unclear. This study reveals a close association between AKAP12 and PDE8A in adult primary cardiomyocytes. Upregulation of AKAP12 in mouse cardiomyocytes significantly diminished contractility and calcium handling. Inhibiting PDE8 in cardiomyocytes with elevated AKAP12 expression enhances contractility downstream of βAR stimulation. This research further demonstrates that AKAP12 upregulation in cardiac tissue accelerates maladaptive remodeling and predisposes the heart to deteriorated cardiac function. Delineating that patients with end-stage heart failure exhibit elevated gene and protein levels of AKAP12 underscores the clinical significance of these findings, emphasizing the novel and impactful nature of this research within the context of heart failure.

Nonstandard Abbreviations and Acronyms

β-AR	β-adrenergic receptor
AC	adenylyl cyclase
AKAP	A-kinase anchoring protein
AKAP12^{ox}	A kinase anchoring protein 12 overexpression
cAMP	cyclic adenosine 3′,5′-monophosphate
cTnI	cardiac troponin-I
ECC	excitation-contraction coupling
GPCR	G-protein coupled receptor
HF	heart failure
LV	left ventricle
PDE	phosphodiesterase
PKA	protein kinase A
PLN	phospholamban
PTX	pertussis toxin
WGA	wheat germ agglutinin
WT	wild type

AKAPs belong to a family of scaffolding proteins that organize complex signal transduction events from the cell membrane–stimulated receptors through recruiting protein kinases, phosphatases, and other signal regulation molecules.[6,7] The structural diversity of AKAPs dictates their scaffolding partners.[6,7] However, all AKAPs have a highly conserved binding domain associated with the regulatory subunit of PKA (protein kinase A).[6,7] To date, several AKAPs have been characterized in the heart, and are associated with cardiac contractility, development, and hypertrophy.[7] Two AKAPs are known to bind directly to β2AR (β2-adrenergic receptor), namely AKAP5 and AKAP12.[8] AKAP5's role in cardiac function has been delineated previously by Nichols et al,[9] who reported that AKAP5 is required for sympathetic stimulation of the calcium transient in cardiomyocytes through scaffolding caveolin-3. On the other hand, AKAP12's importance in cardiac function remains unclear.

AKAP12 (Gravin) is known to scaffold PKA, PDE4D3, PDE4D5, and β2AR.[10–13] To the best of our knowledge, no studies reported that AKAP12 scaffolds to other PDEs. Interestingly, PDE8 is proposed to be located in lipid rafts in human airway smooth muscles, where it specifically regulates β2AR-AC6 signaling and airway remodeling.[14] Our previous study demonstrated that the myristoylation of AKAP12-α at lysine residues is instrumental in directing AKAP12-α:β3-AR:PKA complexes to lipid rafts in adipocytes.[15] Furthermore, PDE8A role in regulating ECC in ventricular cardiomyocytes has been described by Patrucco et al.[16] Given the importance of physical cAMP distribution governed partially by AKAPs in regulating cardiac function, alongside the presence of AKAP12 and PDE8 in lipid rafts across various tissues. This study aimed to investigate whether AKAP12 scaffolds PDE8 in cardiomyocytes, and if increased cardiac AKAP12 expression influences cardiac contractility downstream βAR via the AKAP12-PDE8 axis.

ORIGINAL RESEARCH

METHODS

Data, Materials, and Code Disclosure Statement

All data and materials have been made publicly available using the online figshare data repository and can be accessed at https://doi.org/10.6084/m9.figshare.c.7154392.

Animal Studies

All animal studies have been approved by the Institutional Animal Care and Use Committee (protocol no. 17-017) and the ethics committee at the University of Houston (UH; no. UH-ACP-11-032). Animal care was provided for in AAALAC accredited animal barrier facilities at UH and has therefore been performed in accordance with the ethical standards laid down in the 1964 Declaration of Helsinki and its later amendments. Animal studies have been performed in both males and females 8 to 12 weeks old.

Statistical Analysis

Data were processed using Microsoft Excel (RRID: SCR_016137), Vevo LAB 5.6.1, Image Lab, IonWizard 7.7.1, CytoSolver 3.0, ImageJ, and GraphPad Prism 8.2.1. (RRID: SCR_002798). All values are reported as the mean±SEM. Numeric data were first analyzed for normality using the Shapiro-Wilk test. Data with parametric distribution were analyzed by unpaired 2-tailed Student *t* test and 1-way ANOVA. For multiple comparisons, either the Holm-Sidak or Tukey post hoc multiple comparisons test was used. When significant departures from normality were observed by the Shapiro-Wilk test, nonparametric tests were used. For echocardiograms, 2-way ANOVA and Sidak post hoc multiple comparisons test were used. *P* values of <0.05 were considered significant. Representative images and figures were chosen based on their proximity to the mean/average for each group.

For other materials and methods, please refer to Methods and Materials in the Supplemental Material.

RESULTS

AKAP12 Upregulation Reduces Intracellular cAMP Levels Post–β-Adrenergic Receptor Stimulation

AC16 cells were grouped into cells stably overexpressing AKAP12 (AKAP12-OX), using hygromycin-B selection, or controls (endogenous levels of AKAP12). AKAP12 gene expression levels were significantly higher in the AKAP12-OX group (12.88±2.03, fold change) as compared with controls (1.01±0.07, fold change; $P=4.2\times10^{-3}$; Figure 1A). Protein expression levels were also increased (15.25±1.19, fold change) in the AKAP12-OX group as compared with controls (1.00±0.16, fold change; $P=2.9\times10^{-4}$; Figure 1B and 1C).

In mammalian cells, increased intracellular cAMP levels in cardiomyocytes enhance both the speed (chronotropy) and force (inotropy) of contraction by activating PKA.[17] cAMP production is catalyzed by ACs, which can be activated by the Gαs pathway downstream of stimulated βARs.[17] On the other hand, decreased intracellular cAMP levels can be attributed to either heightened Gαi activity, which inhibits AC, or due to increased degradation of cAMP being catalyzed by PDE.[17,18]

AKAP12 is proposed to scaffold PDE4D and binds to the β2AR.[10,11] Consequently, we anticipated observing lower intracellular cAMP levels in the AKAP12-OX group. To assess this, we utilized the GloSensor-cAMP assay, a luciferase-based biosensor capable of detecting signaling events in real time.

As expected, AKAP12-OX—represented by the red color in this article—had significantly lower intracellular cAMP levels at the point of maximum response accumulation ($[cAMP]_{i\ Max}$; 47.25±13.29,%) compared with controls—represented by the blue color in this manuscript—(86.76±5.30,%; $P=5.3\times10^{-3}$) downstream the stimulated β2AR when treated with 10-μM Epinephrine (Figure 1D).

To investigate if impaired Gαs signaling contributes to the reduced cAMP levels, we directly targeted ACs using 25-μM Forskolin. Results showed that AKAP12-OX had significantly lower $[cAMP]_{i\ Max}$ (38.63±8.72,%) compared with controls (90.49±2.03,%; $P=2.6\times10^{-6}$; Figure S1A). This suggests that the reduced $[cAMP]_{i\ Max}$ in the AKAP12-OX group is not correlated to impaired Gαs pathway activation of ACs. However, this does not exclude the possibility of reduced AC levels in the AKAP12-OX group that could contribute to reduced $[cAMP]_{i\ Max}$ downstream Forskolin.

Higher Gαi activity arises from a combination of increased Gαi protein levels and increased activation of the pathway.[19] Therefore, we pretreated cells with 50-nM PTX (pertussis toxin) overnight before adding 10-μM Epinephrine. PTX pretreatment resulted in significantly lower $[cAMP]_{i\ Max}$ in the AKAP12-OX group (41.92±10.93,%) compared with controls (83.14±6.78,%; $P=3.3\times10^{-2}$; Figure S1B). Western blot analysis indicated comparable Gαi protein expression between the AKAP12-OX and control groups when cells were treated with Epinephrine (0.92±0.08 versus 1.00±0.03, fold change; $P=4.4\times10^{-1}$; Figure S1C). These findings suggest that other factors are likely responsible for decreased $[cAMP]_{i\ Max}$ observed in the AKAP12-OX group.

To study the potential impact of PDEs on $[cAMP]_{i\ Max}$, we pretreated both groups with either 10-μM or 0.1-mM 3-isobutyl-1-methylxanthine (IBMX), a nonselective PDE inhibitor for 30 minutes. Only pretreatment with 0.1-mM (IBMX) followed by 10-μM Epinephrine showed no significant difference in $[cAMP]_{i\ Max}$ between groups; AKAP12-OX (63.99±10.09,%) compared with controls (82.17±5.33,%; $P=4.7\times10^{-1}$; Figure 1E). Although, pretreatment with 10-μM IBMX showed a significantly lower $[cAMP]_{i\ Max}$ in the AKAP12-OX group (48.33±7.46,%) compared with controls (91.27±2.29,%; $P=7.2\times10^{-6}$;

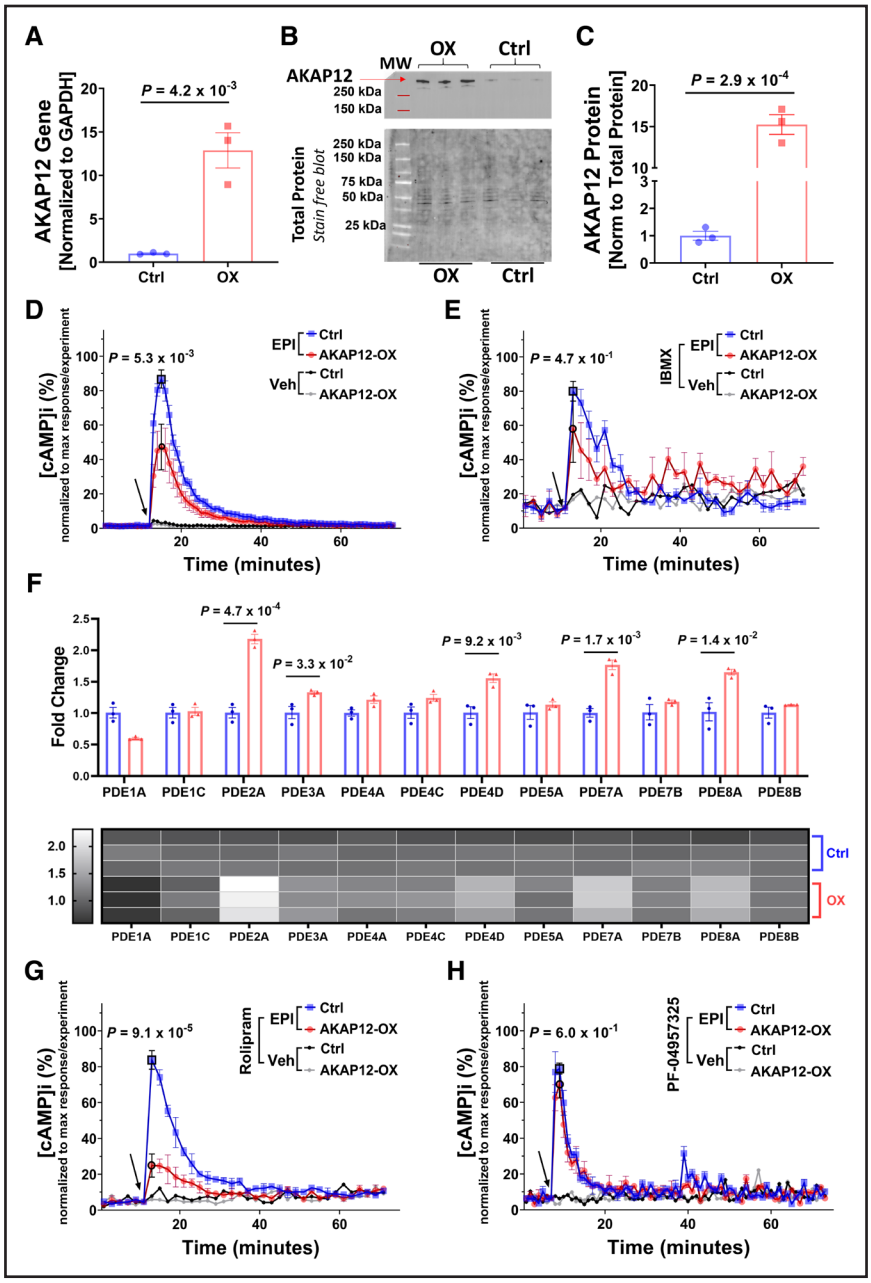

Figure 1. AKAP12 (A kinase anchoring protein 12) upregulation in vitro reduces intracellular cAMP (cyclic adenosine 3′,5′-monophosphate) levels.

A, Quantification of RTqPCR for AKAP12 gene expression in AC16 cells stably transfected with human AKAP12 plasmid (AKAP12-OX) and nontransfected AC16 cells (Ctrl); n=3 in each group. **B**, Representative Western blot comparing AKAP12 expression in AC16 cells stably transfected with human AKAP12 plasmid (AKAP12-OX) and nontransfected AC16 cells (Ctrl). **C**, Quantification of AKAP12 protein expression, n=3 in each group. Intracellular cAMP levels in AC16 cells were detected using Glosensor Luciferase assay under different pretreatments followed by 10-μM Epinephrine (EPI); (**D**) without pre-treatment (**E**) pretreatment for 30 minutes with 0.1-mM IBMX (**G**) pretreatment for 30-minute 10-μM Rolipram, or (**H**) pretreatment for 30-minute 200-nM PF-04957325. **F**, Quantification of RTqPCR for PDEs (phosphodiesterases) in the AC16 cells. Data represented as % intracellular cAMP (normalized data; data was normalized for each experiment separately using the following equation: x new = ((x-x min)/(x max-x min))*100). The arrow indicates the start of EPI treatment or vehicle (Optimem) addition. All data represented as average mean±SEM; **D** and **E**, n=6, (Veh=3 for panel **E**) **G** and **H**; n=3. All experiments were performed as technical duplicates. Data in panels **D**, **E**, **G** and **H** are independent experiments and normalization of data was performed for each treatment separately. Data were determined to have a parametric distribution by the Shapiro-Wilk test; α=0.05 **G**. Data in panels **A**, **C** and **F** were analyzed using unpaired 2-tailed student t-test. Data in panels **D**, **E**, **G** and **H** were analyzed using two-way ANOVA at point of max response followed by Sidak multiple comparisons post hoc test. The point of max response has black borders. Veh indicates vehicle.

Figure S1D). This indicates that decreased $[cAMP]_{i\ Max}$ observed in the AKAP12-OX group could be attributed to elevated PDE activity or increased PDE expression. However, the absence of notable variations in intracellular cAMP levels among the groups during vehicle treatment and before the administration of agonists suggests

that the difference in response to stimulation is unlikely due to alteration in baseline $[cAMP]_{i\ Baseline}$.

Gene expression analysis in the AKAP12-OX group revealed significant upregulation of several PDEs including PDE2A, PDE3A, PDE4D, PDE7A, and PDE8A (Figure 1F). Our attention was particularly directed toward PDE4D and PDE8A among the upregulated PDEs. These 2 enzymes were of interest due to their specificity for cAMP[17] and their potential significance. PDE4D is known for its association with AKAP12,[10] while PDE8A contributes to regulating ECC in cardiomyocytes.[16]

To explore the influence of AKAP12-PDE4 scaffolding on $[cAMP]_{i\ Max}$, we treated cells with the selective PDE4 inhibitor Rolipram (10 μM) for 30 minutes before adding 10-μM Epinephrine. Under Rolipram treatment, the AKAP12-OX group exhibited significantly lower $[cAMP]_{i\ Max}$ (24.83±6.51,%) compared with the controls (83.80±5.19,%; $P=9.1\times10^{-5}$; Figure 1G). These data exclude PDE4 as the main cause of reduced $[cAMP]_{i\ Max}$ in the AKAP12-OX group. Subsequently, we treated cells with the selective PDE8 inhibitor PF-04957325 (200 nM) for 30 minutes before adding 10-μM Epinephrine. Notably, there was no significant difference in $[cAMP]_{i\ Max}$ between the AKAP12-OX group (69.76±7.23,%) and the controls (78.92±3.09,%; $P=6.0\times10^{-1}$; Figure 1H). Based on our present findings, it seems that PDE8 might directly contribute to the reduction of $[cAMP]_{i\ Max}$ in AKAP12-OX groups.

PDE8A Is in the Vicinity of AKAP12 Signalosome in Primary Adult Mouse Cardiomyocytes

Extending our findings to a more physiologically relevant model, we generated a transgenic mouse line that specifically overexpresses AKAP12 in cardiomyocytes ($AKAP12^{OX}$) using an αMHC promoter. We assessed the expression levels of AKAP12 protein in left ventricle (LV) extracts, which confirmed significant upregulation of AKAP12 protein in male mice, with an average expression of (17.25±3.52, fold change) compared with wild-type (WT) male mice (1.00±0.36, fold change; $P=3.7\times10^{-3}$), as well as in female mice, with an average expression of (18.33±3.36, fold change) compared with WT female mice (1.00±0.53, fold change; $P=2.2\times10^{-3}$; Figure 2A and 2B).

After validating our animal model, we investigated $[cAMP]_{i\ Baseline}$ (without ISO) in primary cardiomyocytes isolated from the LV of WT and $AKAP12^{OX}$ mice. ELISA results show no significant differences in $[cAMP]_{i\ Baseline}$ between $AKAP12^{OX}$ males (54.78±3.50 pmol/mL) and WTs (93.51±19.53 pmol/mL; $P=1.2\times10^{-1}$), as well as between $AKAP12^{OX}$ females (63.12±18.75 pmol/mL) and WTs (74.17±22.73 pmol/mL; $P=7.3\times10^{-1}$; Figure 2C and 2D). Gene expression levels of several PDEs and ACs from LV extracts were altered including a significantly upregulated PDE8A in both $AKAP12^{OX}$ males and females compared with WT littermates as well as a significantly downregulated AC8 (Figure S2A and S2B). RNAseq data further support the elevated PDE8A levels (Figure S2C). As such, we expected to observe higher PDE8A protein expression in AKAP12-OX cardiomyocytes. However, WB analysis showed comparable levels in left ventricular extracts from both $AKAP12^{OX}$ and WT groups (Figure S2D and S2E).

Colocalization analysis of AKAP12 and PDE8A showed that Pearson correlation coefficient in the absence of ISO was similar between $AKAP12^{OX}$ cardiomyocytes (0.59±0.05) as compared with WT cardiomyocytes (0.50±0.05; $P=2.7\times10^{-1}$; Figure 2E and 2F). In response to acute βAR stimulation with ISO, PDE8A was colocalized near the cell membrane and AKAP12 to a higher extent in the $AKAP12^{OX}$ cardiomyocytes (0.73±0.04) as compared with WT cardiomyocytes (0.53±0.05; $P=7.2\times10^{-3}$; Figure 2E and 2F). Also, ISO treatment significantly increased AKAP12-PDE8A interaction when compared with no ISO treatment only in the $AKAP12^{OX}$ cardiomyocytes ($P=9.3\times10^{-3}$; Figure 2E and 2F). This indicates that PDE8A is in the vicinity of AKAP12 signalosome, and higher levels of AKAP12 in cardiomyocytes enhance this interaction in response to acute βAR stimulation. Therefore, PDE8A is potentially stabilized within the signalosome which contributes to the reduced cAMP levels near the receptor.

The presence of cAMP is essential for PKA activity, which plays a crucial role in regulating the contraction and relaxation of cardiomyocytes.[20] We assessed PKA activity by examining the levels of cTnI (cardiac troponin-I) phosphorylation in both male and female groups post 14 days ISO treatment. Our results indicate that in post ISO exposure, neither $AKAP12^{OX}$ males (1.09±0.17, fold change) nor $AKAP12^{OX}$ females (0.95±0.17, fold change) showed significantly lower levels of cTnI phosphorylation compared with their WT littermates (2.00±0.27, fold change; $P=4.1\times10^{-1}$) and (0.90±0.41; fold change, $P=9.9\times10^{-1}$), respectively. Similarly, in the absence of ISO exposure, both $AKAP12^{OX}$ males (0.93±0.64, fold change) and females (0.39±0.05, fold change) had comparable phosphorylation of cTnI to their WT littermates (0.94±0.31 and 0.81±0.05, fold change; $P>9.9\times10^{-1}$ and $P=5.8\times10^{-1}$), respectively (Figure S3A and S3B). Although no significant differences in PKA phosphorylation of cTnI were observed between the groups, cardiomyocyte contractility is a multifaceted process controlled by various signaling pathways and cellular components, such as βAR responsiveness, calcium handling, and myofilament sensitivity. Subsequent detailed studies will be conducted to investigate the molecular interplay between AKAP12 and PDE8A, including AC8's role in this context, calcium handling machineries, and myofilament sensitivity.

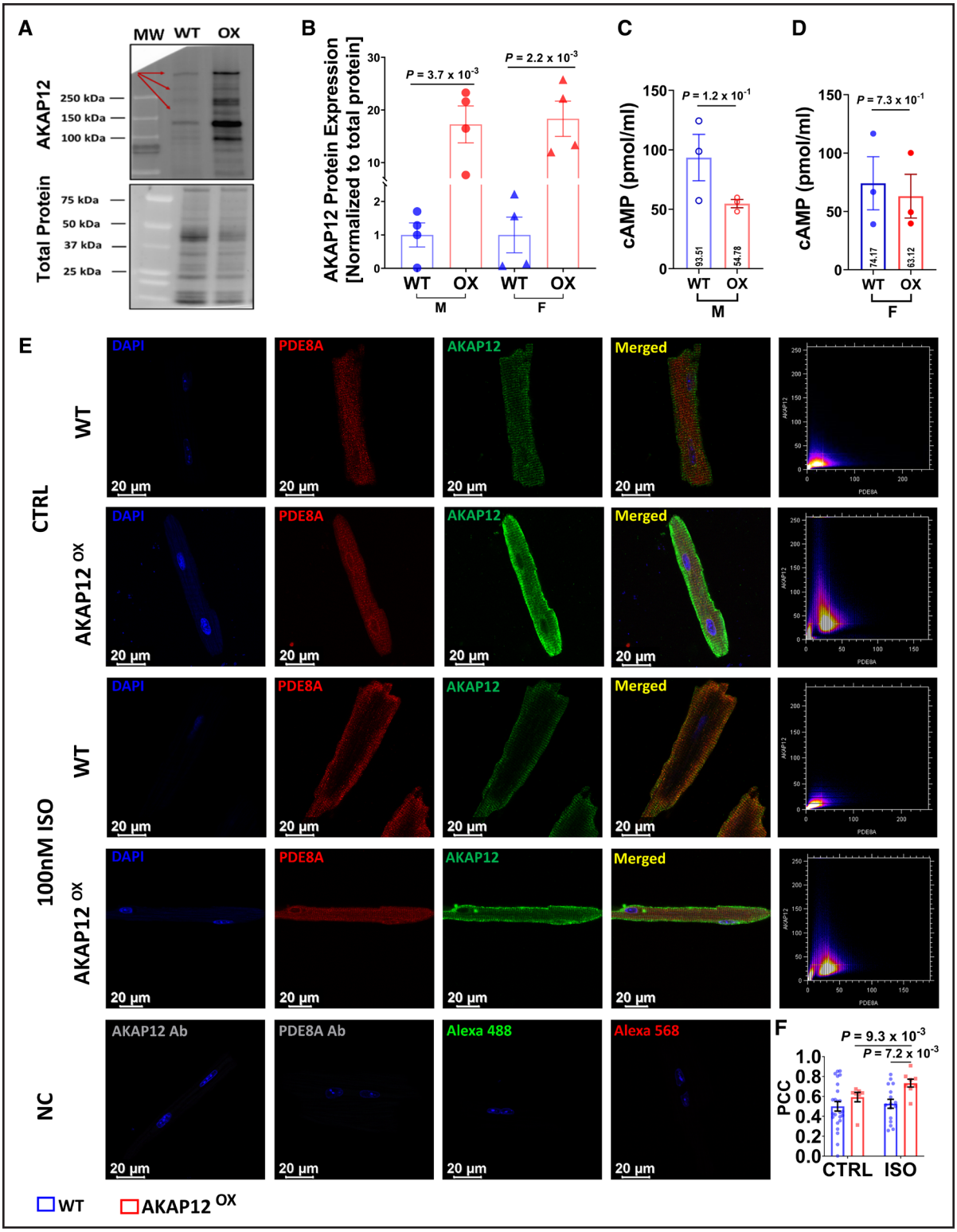

Figure 2. PDE8A (phosphodiestrase 8A) is in the vicinity of the AKAP12 (A kinase anchoring protein 12) signalosome in adult primary cardiomyocytes.

A, Representative Western blot of left ventricular (LV) extracts from mice overexpressing AKAP12 (AKAP12^{OX}) compared with wild-type (WT) littermates. **B**, Quantification of AKAP12 protein levels, N=4 in each group. **C** and **D**, ELISA assay comparing baseline cAMP (cyclic adenosine 3′,5′-monophosphate) levels in primary cardiomyocytes extracted from LVs of AKAP12^{OX} males and female mice, respectively compared with WTs, N=3 in each group. **E**, Representative immunocytochemistry images of primary adult cardiomyocytes and their scatter plot for colocalization using Pearson's correlation test. **F**, Quantification of PDE8A colocalization with AKAP12 in the absence of ISO; n=24 WT, n=7 AKAP12^{OX} and in the presence of ISO; n=16 WT and n=8 AKAP12,^{OX} pooled data. All data represented as average mean±SEM. Data were determined to have a parametric distribution by the Shapiro-Wilk test; α=0.05 and were analyzed using unpaired 2-tailed Student *t* test for all panels except for the AKAP12^{OX} group in **F** which had nonparametric distribution, and data were compared within AKAP12^{OX} group using Mann-Whitney *U* test. NC indicates negative controls.

The remainder of this article will primarily focus on discussing the cellular and physiological consequences of AKAP12 overexpression in cardiomyocytes and its role in cardiac function.

Adult Primary Cardiomyocytes From AKAP12^{OX} Mice Have Reduced Contractility With Acute Isoproterenol Treatment

In presence of ISO, adult primary cardiomyocytes extracted from male AKAP12^{OX} LV had significantly longer sarcomeres at the point of peak contraction — systolic sarcomere length — (1.67±0.02 µm) and significantly reduced % sarcomere shortening (3.69±1.48%) as compared with WT male cardiomyocytes (1.54±0.02 µm; P=4.6×10^{-3}) and (12.03±1.66%; P=9.5×10^{-3}), with no significant differences in resting sarcomere length — diastolic sarcomere length — between the groups (Figure 3A through 3D). AKAP12^{OX} female cardiomyocytes had significantly shorter diastolic sarcomere length (1.75±0.01 µm), longer systolic sarcomere length (1.59±0.01 µm), and reduced % sarcomere shortening (8.99±0.38%) as compared with WT female cardiomyocytes (1.78±0.01 µm; P=3.3×10^{-2}; 1.50±0.03 µm; P=1.6×10^{-2}) and (17.00±0.63%; P=3.7×10^{-5}; Figure 3I through 3L).

Furthermore, AKAP12^{OX} male cardiomyocytes had significantly reduced sarcomere shortening (dL/dt-contraction) and sarcomere re-lengthening (dL/dt-relaxation) absolute rates; (1.50±0.60 and 1.23±0.60 µm/s) as compared with WT males (6.03±1.28 µm/s; P=1.8×10^{-2} and 3.83±0.48 µm/s; P=1.5×10^{-2}; Figure 3E and 3G). A

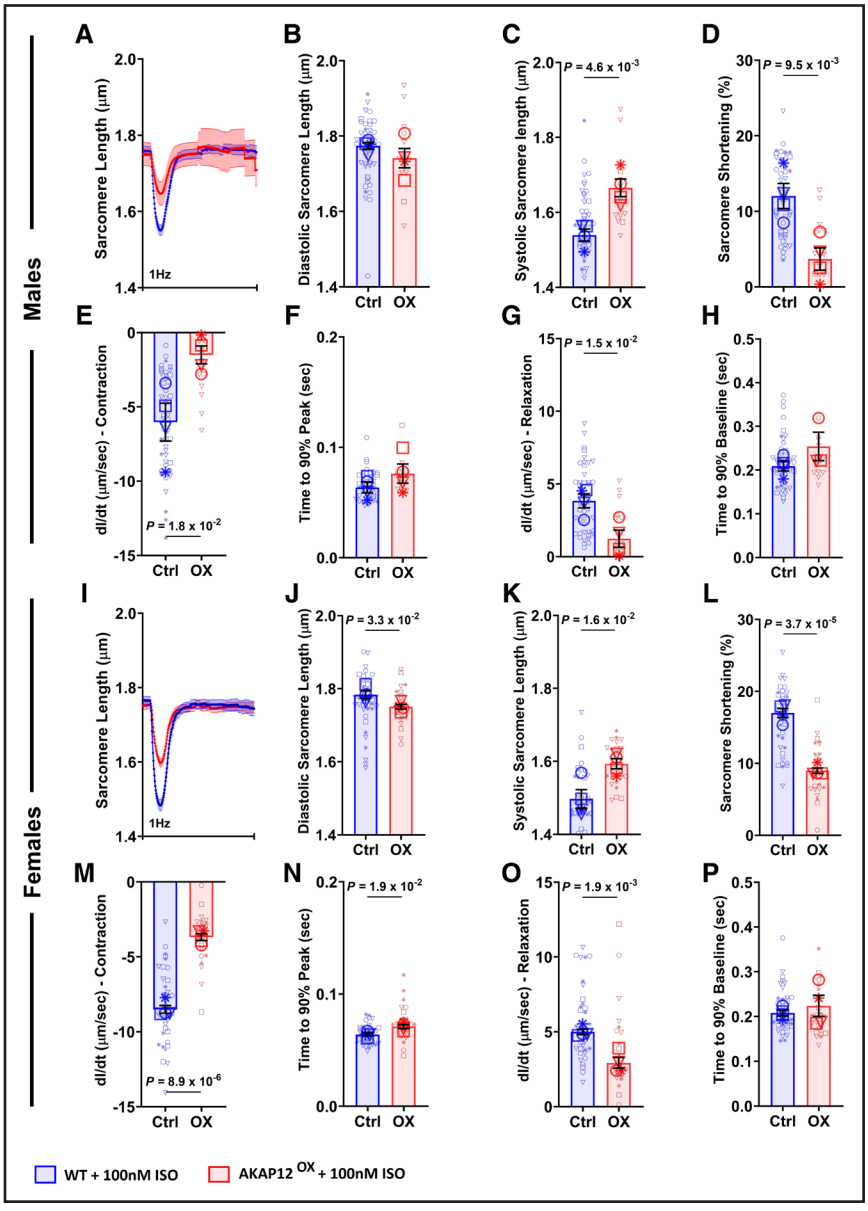

Figure 3. Overexpressing AKAP12 (A kinase anchoring protein 12) in adult primary cardiomyocytes reduces their contractility post acute isoproterenol (ISO) treatment.
A and **I**, Average tracings of sarcomere length from all primary adult cardiomyocytes isolated from male and female mice and treated acutely with ISO. **B** through **H**, Quantification of contractility parameters among the AKAP12^{OX} and wild-type (WT) males, n=49 in WT and n=14-15 in AKAP12^{OX}. **J** through **P**, Quantification of contractility parameters among the AKAP12^{OX} and WT females, n=40-41 in WT and n=26 in AKAP12^{OX}. Comparison of paced cells parameters measured includes (**B** and **J**) diastolic sarcomere length (µm), (**C** and **K**) systolic sarcomere length (µm), (**D** and **L**) sarcomere shortening (%), (**E** and **M**) dl/dt- contraction (µm/s), (**F** and **N**) time to 90% peak (seconds), (**G** and **O**) dl/dt- relaxation (µm/s), and (**H** and **P**) time to 90% baseline (second). All data represented as average mean±SEM of median values for each animal except **A** and **I**, which represents the mean±SEM of all cells. N=4 in each group. Data were determined to have a parametric distribution by the Shapiro-Wilk test; α=0.005 and were analyzed using an unpaired 2-tailed Student *t* test. ‡‡ indicates that the isolation buffer contained Blebbistatin instead of BDM.

similar pattern was observed in AKAP12^{OX} females with dI/dt-contraction and dI/dt-relaxation absolute rates of (3.68±0.23 and 2.92±0.35 µm/s) as compared with WT females (8.51±0.26 µm/s; P=8.9×10^{-6} and 5.00±0.18 µm/s; P=1.9×10^{-3}; Figure 3M and 3O).

In the absence of ISO, AKAP12^{OX} male cardiomyocytes showed no significant differences in systolic and diastolic sarcomere lengths or % sarcomere shortening as compared with WT (Figure S4A through S4D). AKAP12^{OX} female cardiomyocytes had shorter diastolic sarcomere length (1.79±0.01 µm) compared with WT (1.86±0.01 µm; P=2.9×10^{-3}) without any significant differences in systolic sarcomere length or % sarcomere shortening (Figure S4I through S4L). Furthermore, no significant differences were observed in cardiomyocyte dI/dt- contraction and dI/dt- relaxation rates between the groups (Figure S4E, S4G, S4M, and S4O). This suggests a compromised contractile response of the AKAP12^{OX} cardiomyocytes with acute ISO treatment, potentially due to disruptions in the downstream βAR signaling pathways that affect calcium handling. Representative videos of cardiomyocyte contractility with acute ISO treatment in WT (Videos S1 and S2) and AKAP12^{OX} (Videos S3 and S4) groups are available in the Supplemental Material.

Adult Primary Cardiomyocytes From AKAP12^{OX} Mice Have Significantly Higher Basal Intracellular Calcium Levels

Variations in intracellular calcium concentration [Ca^{2+}]i regulate the optimal performance of cardiac contractility by maintaining a sufficiently high [Ca^{2+}]i during systole and a low [Ca^{2+}]i during diastole.[21] Simultaneous to contractility measurements, we investigated [Ca^{2+}]i levels, where we expected to observe significantly lower [Ca^{2+}]i levels in the AKAP12^{OX} cardiomyocytes. Surprisingly, we observed significantly higher resting diastolic (1.10±0.04, F_{340}/F_{380}) and higher peak shortening systolic (2.00±0.16, F_{340}/F_{380}) [Ca^{2+}]i in AKAP12^{OX} female cardiomyocytes post acute ISO treatment compared with WT cardiomyocytes (0.93±0.03, F_{340}/F_{380}; P=1.8×10^{-2}) and (1.54±0.06, F_{340}/F_{380}; P=3.9×10^{-2}); although AKAP12^{OX} male cardiomyocytes were comparable to WT cardiomyocytes (Figure 4A through 4C and 4H through 4J). [Ca^{2+}]i percentage change was not significantly different between AKAP12^{OX} and WT groups, and the elevated systolic calcium did not correlate to enhanced systolic sarcomere shortening in AKAP12^{OX} cardiomyocytes (Figure 4D, 4G, 4K, and 4N). This implies the possibility of different basal [Ca^{2+}]i between the 2 groups.

Indeed, in the absence of ISO, AKAP12^{OX} male and female cardiomyocytes had significantly higher diastolic (1.04±0.07 and 1.16±0.05, F_{340}/F_{380}) and systolic (1.58±0.11 and 1.96±0.21, F_{340}/F_{380}) [Ca^{2+}]i when electrically stimulated compared with cardiomyocytes isolated from WT littermates (0.78±0.02 and 0.90±0.05, F_{340}/F_{380}; P=1.3×10^{-2} and P=7.6×10^{-3}), and (1.12±0.04 and 1.25±0.11, F_{340}/F_{380}; P=8.7×10^{-3} and P=2.5×10^{-2}; Figure S5B through S5D and S5I through S5K). Another distinct difference was the spontaneous calcium release pattern observed only in AKAP12^{OX} cardiomyocytes (Figure 4A and 4H; squared area), which was absent without ISO treatment (Figure S5A and S5H), indicating irregular calcium handling in the AKAP12^{OX} cardiomyocytes downstream of the βARs stimulation.

Next, we investigated [Ca^{2+}]i and contractility in cardiomyocytes downstream β1AR versus β2AR separately, which showed different patterns in response to acute stimulation by ISO. β1AR stimulation with ISO—while blocking β2AR with 50-nM ICI-118 551—showed no significant differences in % shortening or % [Ca^{2+}]i change in either AKAP12^{OX} males or females isolated cardiomyocytes as compared with the WT cardiomyocytes (Figure S6A through S6C and S6G through S6I).

During β2AR stimulation with ISO—while blocking β1AR with 100-nM CGP 20712A—we observed the percentage shortening in AKAP12^{OX} males (1.90±0.60%) was significantly lower as compared with the WT cardiomyocytes (5.06±0.70%; P=2.7×10^{-2}) despite the comparable [Ca^{2+}]i % change in the AKAP12^{OX} group (28.15±4.42%) as compared with WT cardiomyocytes (29.23±2.26%; P=8.4×10^{-1}; Figure S6D through S6F). On the other hand, AKAP12^{OX} females had a comparable % shortening (6.76±1.39%) to WTs (6.01±2.51%, P=8.1×10^{-1}) despite the significantly higher [Ca^{2+}]i percentage change in the AKAP12^{OX} group (41.32±5.85%) as compared with WTs (23.05±0.85%; P=3.7×10^{-2}; Figure S6J through S6L). Together, this indicates that downstream β1AR signaling in AKAP12^{OX} and WT cardiomyocytes respond similarly. Whereas downstream β2AR signaling, AKAP12^{OX} cardiomyocytes demonstrate impaired contractility to similar [Ca^{2+}]i, or fail to enhance contractility at higher [Ca^{2+}]i compared with WT cardiomyocytes.

The latter response observed is similar to the response when both βARs are activated by ISO, specifying that AKAP12 mediates its effect through β2AR.

PDE8 Inhibitor (PF-04957325) Reverses AKAP12^{OX} Effect on [Ca^{2+}]i and Contractility in Adult Primary Mouse Cardiomyocytes

In the absence of ISO and PF-04957325, sarcomere shortening % in AKAP12^{OX} males and females cardiomyocytes (3.24±0.80% and 4.50±0.56%) was comparable to WT cardiomyocytes (2.86±0.28% and 3.72±0.46%; P=5.70×10^{-1} and P=2.3×10^{-1}), respectively. The addition of 30-nM PF-04957325 increased

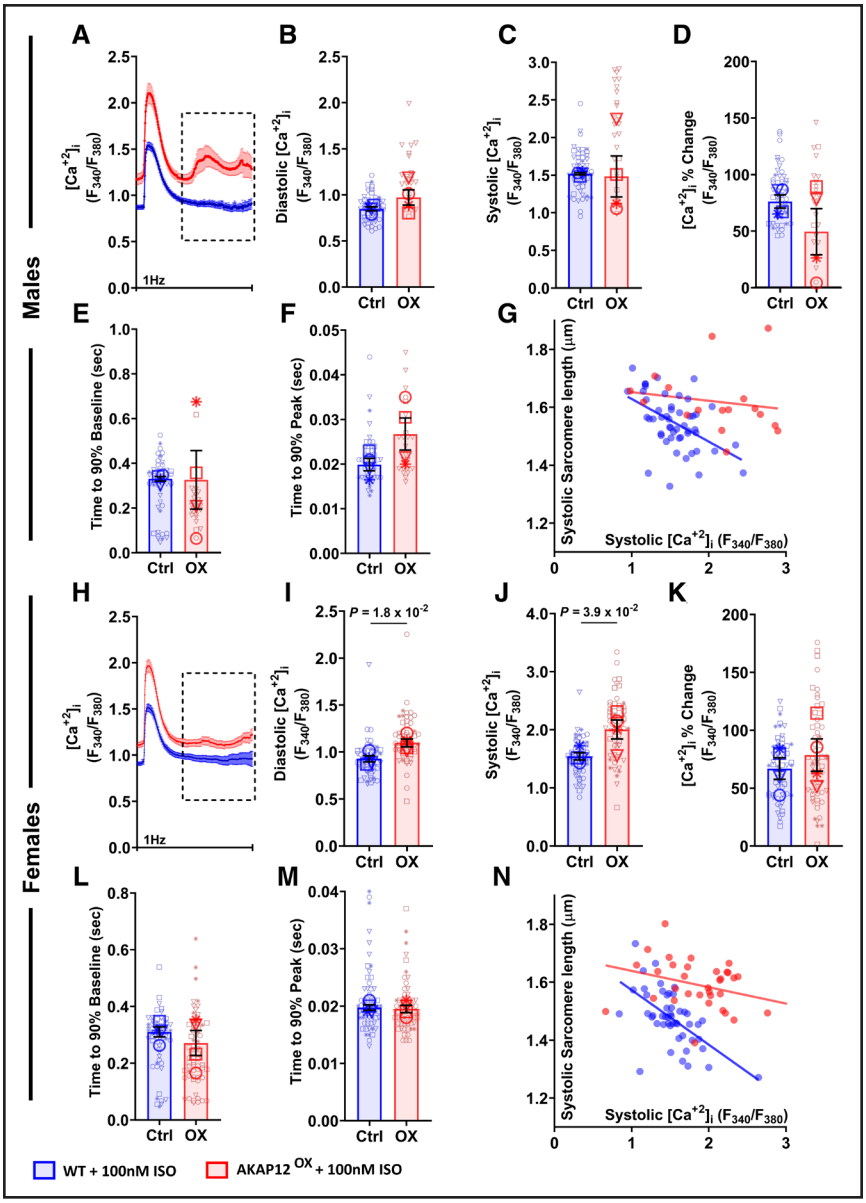

Figure 4. Overexpressing AKAP12 (A kinase anchoring protein 12) in adult primary cardiomyocytes significantly increases intracellular calcium post acute isoproterenol (ISO) treatment. **A** and **H**, Average tracings of $[Ca^{2+}]i$ represented by Fura-2 fluorescence ratio (340 nm/380 nm) from all primary adult cardiomyocytes isolated from male and female mice treated acutely with ISO. **B** through **F**, Quantification of $[Ca^{2+}]i$ and calcium kinetics among the AKAP12^{OX} and wild-type (WT) males; n=52 in WT and n=24 in AKAP12^{OX}. **I** through **M**, Quantification of $[Ca^{2+}]i$ and calcium kinetics among the AKAP12^{OX} and WT females; n=59 in WT and n=64 in AKAP12^{OX}. Comparison of paced cells parameters measured includes **B** and **I**, diastolic $[Ca^{2+}]i$ (F340/F380); **C** and **J**, systolic $[Ca^{2+}]i$ (F340/F380); **D** and **K**, $[Ca^{2+}]i$ change (%; E and L) time to 90% baseline (seconds); **F** and **M**, time to 90% peak (seconds). **G** and **N**, Scatter plot of systolic $[Ca^{2+}]i$ (F_{340}/F_{380}) and systolic sarcomere length (µm). N=4 in each group. All data represented as average mean±SEM of median values for each animal except **A** and **H**, which represents the mean±SEM. of all cells. Data were determined to have a parametric distribution by the Shapiro-Wilk test; α=0.005 and were analyzed using an unpaired 2-tailed Student *t* test. ‡‡ indicates that the isolation buffer contained Blebbistatin instead of BDM.

sarcomere shortening %, but the difference was not statistically significant compared with the baseline in any of the groups (Figure 5A and 5D). However, the subsequent introduction of 100-nM ISO, alongside 30-nM PF-04957325, resulted in a significant increase in sarcomere shortening % within each group compared with their baseline and 30-nM PF-04957325 alone (Figure 5A and 5D). Notably, in the presence of both PF-04957325 and ISO, both male and female AKAP12^{OX} cardiomyocytes exhibited significantly higher sarcomere shortening % (10.31±1.18% and 11.79±1.10%) compared with WT cardiomyocytes (7.66±0.66% and 6.39±0.56%; P=4.8×10^{-2} and P=2.2×10^{-5}; Figure 5A and 5D).

While 30-nM PF-04957325 alone did not significantly impact $[Ca^{2+}]i$ in either male or female AKAP12^{OX} or WT cardiomyocytes compared with their baseline $[Ca^{2+}]i$, the combination of 30-nM PF-04957325 and 100-nM ISO led to a significant increase in $[Ca^{2+}]i$ within each group compared with their baseline and 30-nM PF-04957325 alone (Figure 5B and 5E). In the presence of both PF-04957325 and ISO, both male and female AKAP12^{OX} cardiomyocytes had a significantly higher % $[Ca^{2+}]i$ change (59.21±7.12% and 72.65±8.25%) compared with WT cardiomyocytes (39.26±3.88% and 19.76±2.70%; P=1.6×10^{-2} and P=7.2×10^{-9}; Figure 5B and 5E). The enhanced $[Ca^{2+}]i$ in the AKAP12^{OX} group showed better contractility (Figure 5C and 5F). This unique response further strengthens the evidence supporting the hypothesis of the AKAP12^{OX}–PDE8 axis in regulating ECC.

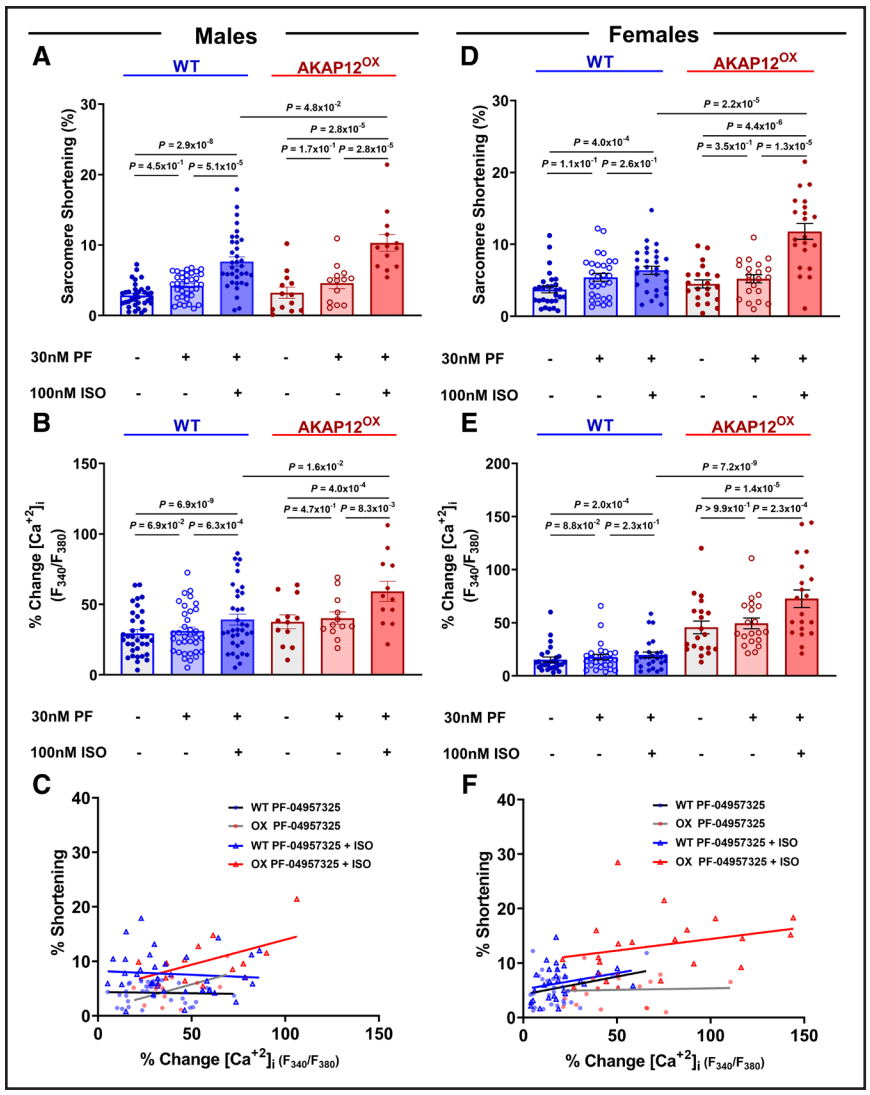

Figure 5. PDE8 (phosphodiesterase 8) inhibitor (PF-04957325) reverses AKAP12^{OX} effect on [Ca^{2+}]i and contractility in primary adult mice cardiomyocytes.
A through **C**, Quantification of PDE8 inhibition effects on cardiomyocytes calcium and contractility and their scatter plot among the AKAP12^{OX} and wild-type (WT) males; n=35 in WT and n=12-13 in AKAP12^{OX}. **D** through **F**, Quantification of PDE8 inhibition effects on cardiomyocytes calcium and contractility and their scatter plot among the AKAP12^{OX} and WT females; n=27-29 in WT and n=20-21 in AKAP12^{OX}. N=3 to 4 in each group. When data were determined to have a parametric distribution by the Shapiro-Wilk test; α=0.05, AKAP12^{OX} groups in **D** and **B**, 1-way ANOVA was used to assess data within each group. Other data with nonparametric distribution were compared within each group using the Friedman test. Mann-Whitney *U* test was used to compare PF-04957325+ISO effects between groups in all except **A**; unpaired 2-tailed Student *t* test. ISO indicates isoproterenol; and PF; PF-04957325.

Cardiac AKAP12^{OX} Upregulates Maladaptive Genes in the LV Following 14-Day Isoproterenol Treatment

To address how cardiac AKAP12^{OX} would affect cardiac function post 14 days ISO treatment, we performed RNAseq analysis on LV extracts from AKAP12^{OX} and WT mice exposed to ISO for 14 days as well as from sham mice (no exposure to ISO).

RNAseq data show that treatment with ISO significantly upregulated 9 of the known maladaptive genes in AKAP12^{OX} females (NPPA, GRK5, CTGF, NPPB, P4HA1, LOXL4, TGFB2, NOX4, and SFRP1) and 12 maladaptive genes in AKAP12^{OX} males (NPPA, NPPB, GRK5, CTGF, THBS4, POSTN, LOXL4, TGFB2, NOX4, SFRP1, P4HA1, and FBLN2) as compared with WT littermates exposed to ISO (Figure 6). Furthermore, AKAP12^{OX} sham mice upregulated some maladaptive genes, such as NPPA, CTGF and NPPB. (Figure 6). Notably, AKAP12^{OX} mice upregulated some adaptive genes as well, such as WISP2, FRZB, and FSTL1 as compared with WT littermates (Figure 6). However, the extent of upregulation observed for the maladaptive genes was higher compared with the average upregulation seen for adaptive genes in the AKAP12^{OX} group (Figure S7). This suggests that AKAP12^{OX} might predispose LV tissue to faster remodeling, lower contractility, and systolic malfunction with prolonged ISO treatment. Please refer to the online figshare data repository for detailed *P*-values of maladaptive genes comparisons after ISO treatment.

Cardiac AKAP12^{OX} Worsens Cardiac Systolic Function and Promotes Left Ventricular Hypertrophy Post 14 Days of Isoproterenol Treatment

To confirm that AKAP12^{OX} might impair ventricular contractility, we examined cardiac function in AKAP12^{OX} males and females, compared with WT controls, after treatment with 60 mg/kg per day of ISO for 14 days.

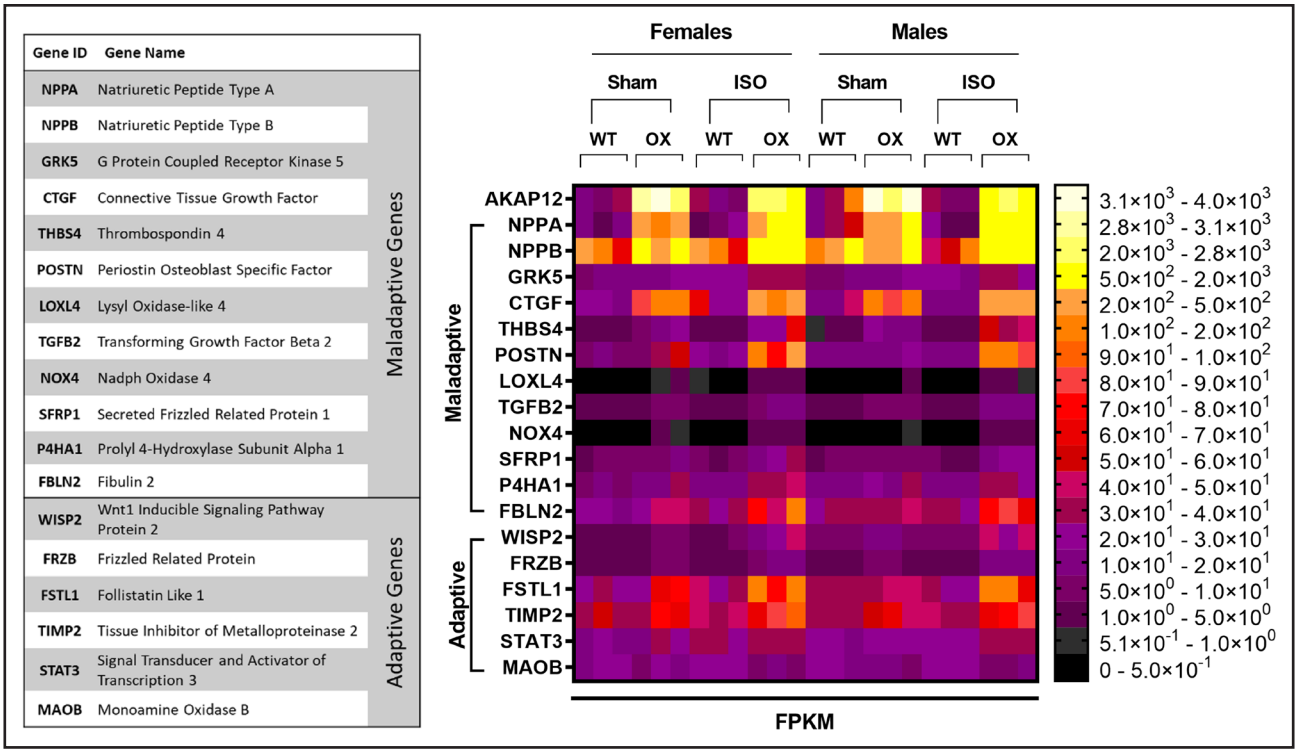

Figure 6. Cardiomyocytes AKAP12^{OX} upregulates maladaptive genes in the left ventricle (LV).
Heat map of maladaptive and adaptive gene expression (FPKM [fragments per kilobase of exon per million mapped fragments]), assessed in LV extracts from AKAP12^{OX} and wild-type (WT) male and female mice (8–12 weeks old) in the absence of isoproterenol (ISO) treatment (Sham) and after 14 days post-isoproterenol treatment (ISO); N=3 in each group.

In the WT groups, we noticed that the Ejection Fraction % (EF%) and Fractional Shortening % (FS%) showed divergent responses after 14 days of treatment with 60 mg/kg per day of ISO; where some mice exhibited an increase in EF% and FS% while others experienced a decrease, aligning with prior findings with variable ISO doses.[22–24] However, all male and female AKAP12^{OX} mice demonstrated reduced EF% and FS% after the 14-day treatment period (Figure 7A, 7B, 7E, and 7F).

Precisely, both male and female AKAP12^{OX} mice had significantly lower EF% (42.97±5.78% and 43.89±3.61%) as compared with WT littermates post-ISO treatment (65.22±4.07% and 57.39±3.95%; P=9.9×10^{-3} and P=3.5×10^{-2}), respectively. Furthermore, male AKAP12^{OX} mice had significantly lower FS% (21.38±3.53%) as compared with WT littermates (36.21±3.40%; P=2.8×10^{-2}) post 14 days ISO treatment (Table S1; Figure 7). Global circumferential strain showed significantly lower LV systolic shortening in both AKAP12^{OX} males and females post-ISO treatment (−7.81±0.76 and −14.45±2.22) as compared with WT males and females (−19.28±2.13 and −23.24±2.79; P=2.5×10^{-3} and P=3.9×10^{-2}), respectively (Figure 7C and 7G). Representative videos of global circumferential strain for WT (Video S5) and AKAP12^{OX} (Video S6) are available in Supplemental Material. Importantly, neither 14 days of vehicle (0.002% ascorbic acid) treatment, nor sham conditions showed a significant difference in systolic cardiac parameters; EF% and FS% between AKAP12^{OX} and WT groups after 14 days of ISO treatment (Figure S8; Tables S2 through S5). For detailed statistical analysis for sham, vehicle-treated, or ISO-treated groups, please refer to Supplemental Raw Data D1 through D3.

LV hypertrophy was assessed using a corrected LV mass to body weight ratio, and WGA (wheat germ agglutinin) to determine cross-sectional area of cardiomyocytes in cardiac sections. AKAP12^{OX} males and females post 14 days of ISO treatment had higher LV mass/body weight (7.12±0.52 and 10.51±1.09 mg/g) as compared with WT littermates (5.50±0.59 and 6.40±0.77 mg/g; P=8.0×10^{-2} and P=8.6×10^{-3}), respectively (Table S1; Figure 7D and 7H). WGA staining further confirmed that 14 days post-ISO treatment AKAP12^{OX} cardiomyocytes from both males and females had significantly higher cross-sectional area (546.90±20.95 and 463.0±15.81 μm^2) as compared with WT cardiomyocytes (241.40±9.59 and 260.5±7.81 μm^2; P=1.0×10^{-15} and P=1.0×10^{-15}), respectively (Figure 7I through 7K). In the absence of ISO, male and female AKAP12^{OX} cardiomyocytes still had significantly higher cross-sectional area (227.0±9.79 and 193.7±7.20 μm^2) as compared with WT cardiomyocytes (137.6±3.80 and 121.8±4.33 μm^2; P=5.6×10^{-6} and P=2.0×10^{-6}). These results suggest that AKAP12^{OX} cardiomyocytes are predisposed to

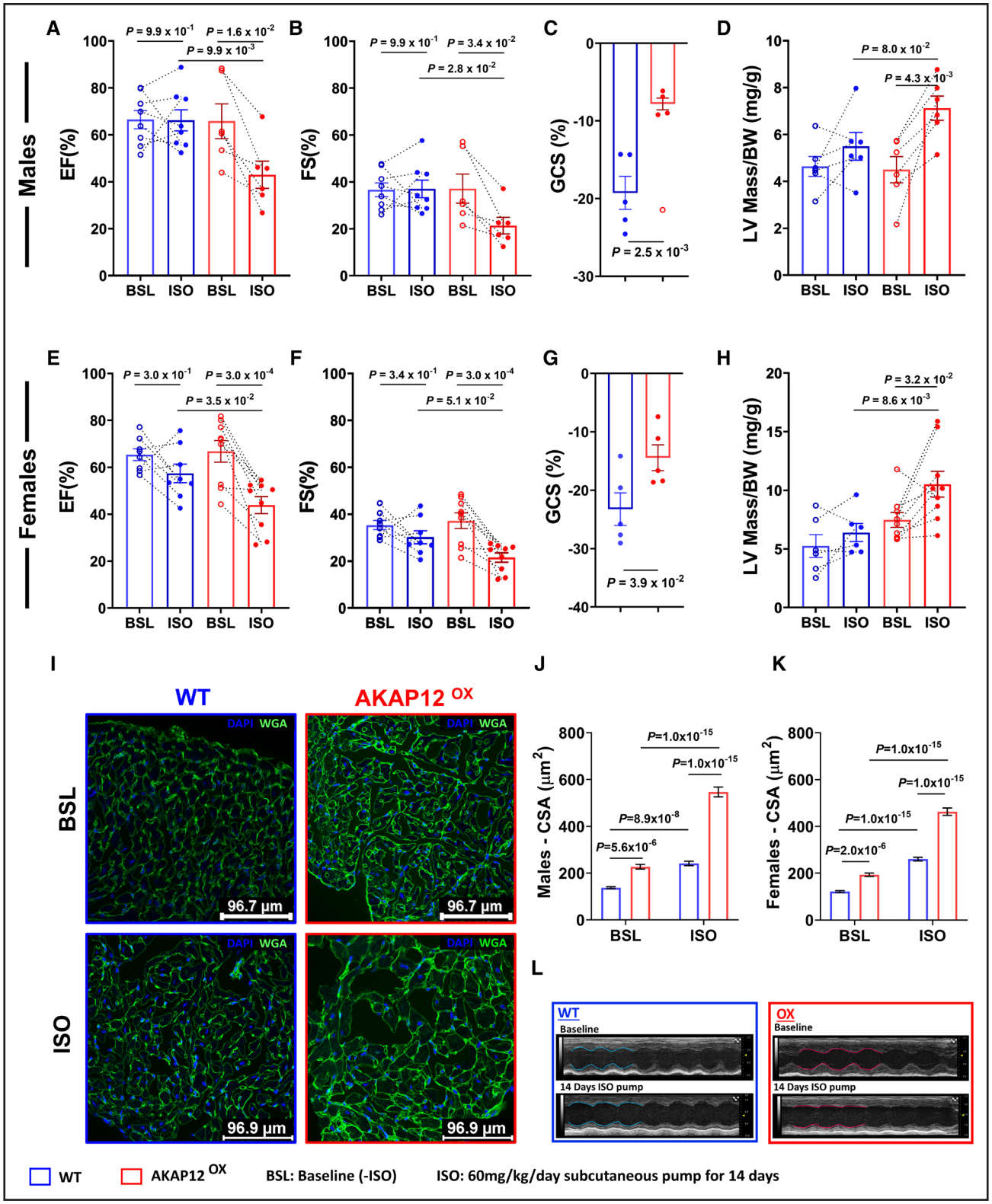

Figure 7. Cardiac AKAP12^{OX} worsens systolic function and promotes left ventricular hypertrophy.
A through **C**, Echocardiographic measurements of systolic cardiac function before and after 14 days of isoproterenol (ISO) treatment in AKAP12^{OX} and wild-type (WT) males; N=9 in WT and N=6 in AKAP12^{OX}. Comparison of parameters measured includes **A**, ejection fraction (%), **B**, fractional shortening (%), and **C**, global circumferential strain (%); N=5 in each group. **D**, Left ventricular (LV) hypertrophy measurement represented by corrected LV mass/body weight ratio before and after ISO treatment; N=6 in each group. **E** through **G**, Echocardiographic measurements of systolic cardiac function before and after 14 days of ISO treatment in AKAP12^{OX} and WT females; N=8 in WT and N=9 in AKAP12^{OX}. Comparison of parameters measured include **E**, ejection fraction (%), **F**, fractional shortening (%), and **G**, global circumferential strain (%); N=5 in each group. **H**, LV hypertrophy measurement represented by corrected LV mass/body weight ratio before and after ISO treatment; (*Continued*)

hypertrophy independently of ISO stimulation, and are more susceptible to hypertrophic stimuli, such as ISO.

AKAP12 Is Upregulated in the LVs of Patients With End-Stage HF

Based on our in vivo experiments, and previous transcriptomic studies reported in the ReHEAT database[25] showing altered levels of AKAP12 in patients with HF (Figure 8A), we were interested in evaluating whether AKAP12 is upregulated in LV extracts from patients with end-stage HF (Table S6). In failing hearts (F, n=8), AKAP12 gene expression was (2.91±0.55) as compared with nonfailing hearts (NF, n=6) at (1.05±0.13, fold change; P=1.4×10^{-2}; Figure 8B). AKAP12 protein expression had a similar pattern in failing hearts (2.01±0.15) compared with nonfailing hearts (1.00±0.21, P=1.6×10^{-3}; Figure 8C and 8D).

Collectively, our data strongly suggest that AKAP12 upregulation is associated with impaired cardiac function.

DISCUSSION

Cardiac function is mainly mediated by the β-adrenoceptor stimulation and subsequent production of the second messenger cAMP.[1,20] cAMP regulates cardiomyocyte contractile function through activating PKA.[20] Constant high levels of cAMP in cardiomyocytes can induce cardiac remodeling and hypertrophy.[26] On the other hand, persistent lower cAMP levels are considered a hallmark of maladaptive cardiac remodeling.[27] Thus, for optimal cardiac function cAMP levels are tightly controlled by balancing cAMP production and degradation.[18]

Although both βARs stimulate cAMP production, cells differently interpret the signal produced by the 2 receptor subtypes: β1AR and β2AR.[28,29] These differences are partially attributed to the variable cAMP distribution patterns, which historically were associated with the receptor expression patterns; global cAMP increase downstream β1AR (globally expressed on cardiomyocyte's surface), and localized cAMP increase downstream the β2AR (localized to the caveola).[30]

Currently, it is recognized that AKAPs compartmentalize cAMP signals forming microdomains of the second messenger within the cell in a stimulus-induced manner, assuring some level of specificity.[31–33] To date, several AKAPs have been associated with cardiac development, contractility, cardiac morphology, and rhythm.[34–43] AKAP12 is known to scaffold PKA, PDE4D3, PDE4D5, and β2AR; hence, it assembles a signalosome that can regulate cAMP levels downstream or near the β2AR.[10–13] However, AKAP12's role in cardiac contractility post acute and chronic stimulation of βAR is still unclear. Considering the importance of intracellular cAMP levels for cardiac contractility, we investigated how AKAP12 upregulation in vitro affected the intracellular cAMP levels in real-time post-β2AR stimulation.

In our molecular model using the AC16 cells, we observed that AKAP12 upregulation significantly reduced $[cAMP]_{i\ Max}$ compared with controls when treated with Epinephrine, which we concluded is regulated through AKAP12-PDE8 interplay. The PDE family includes 11 members out of which 7 are expressed in heart and can be divided into (1) cAMP-specific: PDE4 and PDE8 (2) cGMP specific: PDE5, and (3) dual-specificity: PDE1, PDE2, PDE3 and PDE11.[44] Pretreatments with Rolipram (a selective PDE4 inhibitor) showed significant $[cAMP]_{i\ Max}$ in the AKAP12-OX group compared with controls. Only when using 0.1-mM IBMX (a nonselective PDE inhibitor); $[cAMP]_{i\ Max}$ were not significantly different between AKAP12-OX and controls. However, pretreatment with 10-μM IBMX resulted in significantly lower $[cAMP]_{i\ Max}$ in the AKAP12-OX group as compared with controls. The higher IBMX concentration effectively inhibits cAMP degradation by PDEs, masking the cAMP differences between AKAP12-OX and controls. In contrast, at lower IBMX concentrations, the impact of AKAP12-OX on cAMP levels becomes discernible due to less pronounced PDE inhibition. Additionally, the presence of comparable $[cAMP]_{i\ Max}$ in AKAP12-OX groups and controls due to the selective PDE8 inhibitor; PF-04957325 strongly implies a central role played by PDE8 in the reduction of $[cAMP]_{i\ Max}$ observed in AKAP12-OX.

A previous study proposed that PDE8A directly binds the PKA-RIα subunit.[45] Most AKAPs including AKAP12 preferentially bind to PKA-RII.[7] However, there is a possibility that AKAP12 also binds to the PKA-RI subunit; hence, AKAP12 might bind to or be in proximity to PDE8A. We speculated that AKAP12 regulates cAMP levels near β2AR by interacting with PDE8A and stabilizing it within the signalosome. In the absence of ISO, immunocytochemistry results from AKAP12^{OX} and WT primary cardiomyocytes showed a similar pattern of PDE8A distribution in the cytoplasm while treatment with 100-nM ISO recruited PDE8A to the cell membrane, a

Figure 7 Continued. N=6 in WT and N=9 in AKAP12^{OX}. **I**, Representative immunocytochemistry images of WGA staining in cardiac slices before and after ISO treatment to assess cardiac hypertrophy through the cross-sectional area. **J** and **K**, Quantification of the cross-sectional area of cells in males and females cardiac slices respectively; n=90, N=3 in each group. **L**, Representative echocardiogram images. All data represented as average mean±SEM. Data were determined to have a parametric distribution by the Shapiro-Wilk test except panels J&K which had non parametric distribution. Two-way ANOVA was used for data comparison in all except **C** and **G**, which were evaluated using unpaired 2-tailed Student *t* test. Sidak post hoc multiple comparison test was used for panels **A**, **B**, **D**, **E**, **F** and **H** while Tukey post hoc multiple comparison test was used for panels **J** and **K**. **C**, A red circle without filling is an excluded outlier, detected using the ROUT (robust regression and outlier removal) method; Q=2% and was not used in the statistical analysis.

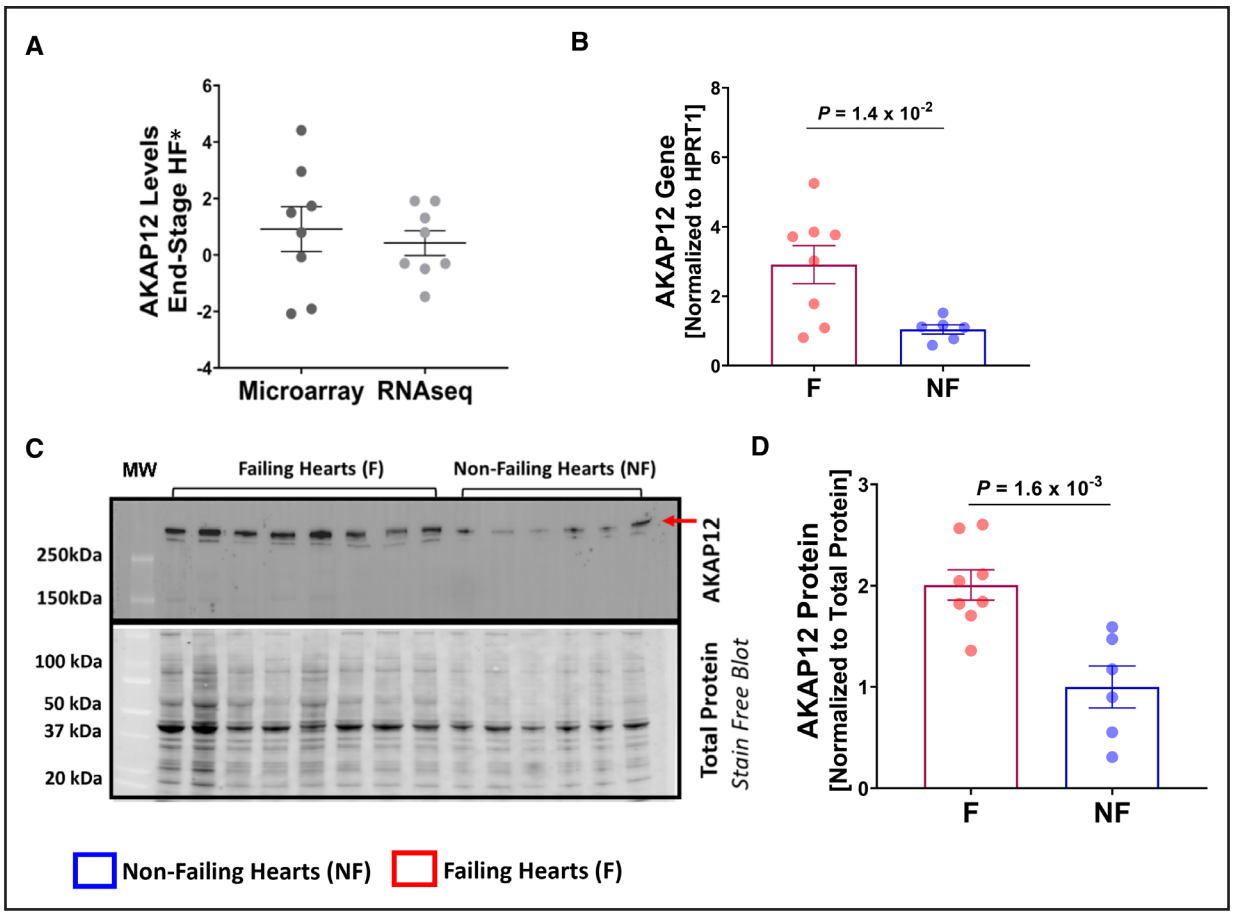

Figure 8. AKAP12 gene and protein expression are upregulated in human failing hearts.
A, Summary plot of AKAP12 gene expression data that was generated from a previous report of 16 meta-studies,[25] each point represents average expression from 1 study represented as t-value resulting from the individual differential expression analysis. **B**, Quantification of AKAP12 gene expression in left ventricular (LV) samples collected from patients with failing hearts; n=8 and nonfailing hearts; n=6. **C**, Western blot of AKAP12 including all LV samples collected from patient failing and nonfailing hearts. **D**, Quantification of the Western blot failing hearts; n=8 and nonfailing hearts; n=6. All data represented as average mean±SEM. Data were determined to have a parametric distribution by the Shapiro-Wilk test; α=0.05 and were analyzed using unpaired 2-tailed Student *t* test for all panels.

pattern reported in other PDEs.[46] PDE8A colocalized with AKAP12 near the cell membrane irrespective of the presence or absence of βAR stimulation with ISO. Higher colocalization, especially with ISO stimulation was observed in the AKAP12^{OX} cardiomyocytes. These findings directly support AKAP12-PDE8A interaction in cardiomyocytes underscoring the significance of PDE8 as a local cAMP modulation target within the AKAP12 signalosome prompting further inquiry into its impact on cardiac contractility.

βARs regulate ECC through cAMP, β1AR is the main regulator of cardiac contractility where its stimulation elicits global elevation in cAMP levels; although β2AR stimulation is known to increase local cAMP levels.[29] Research suggests that β1AR regulation of contractility is cAMP-dependent while β2AR regulation is cAMP-independent.[29] However, it is unclear whether β2AR cardiomyocyte regulation is truly cAMP-independent. In our study, under β1AR selective stimulation, AKAP12^{OX} and WT cardiomyocytes showed similar contractility to comparable [Ca^{2+}]i. In contrast, selective β2AR stimulation showed that AKAP12^{OX} cardiomyocytes had lower contractility in the presence of significantly higher [Ca^{2+}]i as compared with WT. This pattern was also observed when both βARs were stimulated with the nonselective βAR agonist, ISO suggesting that AKAP12 modulates cardiomyocytes ECC through β2AR. Cardiomyocyte contraction kinetics further show a pattern of augmented β2AR signaling.[29] This was observed by a significantly reduced cardiomyocyte contractile shortening response in AKAP12^{OX}, as compared with ISO-treated WTs.

If AKAP12^{OX} enhances signaling downstream of β2AR in cardiomyocytes, one might initially anticipate an improvement in cardiac function due to the well-established cardioprotective effects of β2AR, as suggested in the literature.[47] However, it seems that the impact of the β2AR subtype on cardiotoxic versus cardioprotective signaling is heavily influenced by the type, duration, and intensity of cardiac stress. This observation stems from a study indicating that ablation of β2AR had

a cardioprotective effect in TAC-induced HF, leading to the restoration of Ca^{2+} handling and improved contractility.[48] This finding supports our β2AR results where their stimulation in AKAP12^{OX} mice had a negative influence on contractility, and blocking β2AR results in comparative % $[Ca^{2+}]$i and contractility between groups.

One interpretation of this augmented β2AR's regulation of contractility is that AKAP12, which regulates cAMP locally near β2AR, when overexpressed in cardiomyocytes forms a significantly higher number of intracellular microdomains that contain PDE8. Upon βAR stimulation, a greater cohort of these domains is recruited near the cell membrane, reducing intracellular cAMP levels in many local domains. This may resemble a global reduction in cAMP, which is pivotal for the cAMP-dependent β1AR regulation of contractility, without affecting the cAMP-independent β2AR regulation of contractility. Alternatively, AKAP12 upregulation may directly contribute to increased PDE8 activity resulting in significantly lower cAMP levels that reduce contractility, which we aim to address in our future studies in more detail.

Patrucco et al[16] reported that loss of PDE8A activity in genetically modified mice leads to increased βAR-mediated Ca^{2+} transients and enhanced activation of L-type Ca^{2+} channels suggesting that PDE8A serves as an important acute regulator of $[Ca^{2+}]$i levels during cardiac contraction. This aligns with our findings, showing significantly enhanced % change in $[Ca^{2+}]$i levels and contractility in AKAP12^{OX} cardiomyocytes compared with WT cardiomyocytes only observed in the presence of both PDE8A inhibitor PF-04957325 and ISO stimulation. Additionally, Grammatika Pavlidou et al[49] recently established that PDE8B is a novel regulator of atrial arrhythmogenesis by regulating Ca^{2+} handling. Although we studied the PDE8A isoform, our findings also showed altered Ca^{2+} handling such as the elevated diastolic $[Ca^{2+}]$i in AKAP12^{OX} cardiomyocytes in the presence or absence of ISO treatment, which may be regulated through cAMP/PKA axis. Despite the observed comparable cardiac troponin-I phosphorylation, our preliminary study showed differences in PLN (phospholamban) phosphorylation patterns within a small cohort of AKAP12^{OX} and WT mice pointing to the possibility that AKAP12 regulates PLN (data not shown). Whether this is through the PKA axis or through its interaction with AKAP7 (AKAP18), which is known to scaffold PLN,[50] is unknown. We also observed an irregular beating pattern only in the presence of ISO treatment which will be further analyzed to detect any arrhythmogenicities in AKAP12^{OX} cardiomyocytes.

Based on this, a deteriorated cardiac function in AKAP12^{OX} mice was expected compared with the WT mice post 14 days ISO treatment. To promote cardiac remodeling, we used subcutaneous osmotic pumps that delivered 60 mg/kg per day of ISO for 14 days. ISO-treated WT males and females underwent cardiac remodeling as observed by the significant LV hypertrophy compared with baseline groups. Some WT males and females showed elevation in EF% and FS% while others showed reduced EF% and FS%, which have been reported by others in previous studies.[28–30] In contrast, ISO-treated AKAP12^{OX} males and females had undergone significantly higher cardiac remodeling compared with WT ISO-treated groups. Additionally, AKAP12^{OX} mice showed significantly reduced EF% and FS% compared with WT ISO-treated groups. Considering that 60 mg/kg per day ISO dose did not deteriorate cardiac function in WT mice in this study indicates that AKAP12^{OX} mice indeed are more prone to cardiac dysfunction with 14 days ISO treatment. Further support of this notion is the upregulation of maladaptive genes to a higher extent in the AKAP12^{OX} mice.

Consequently, we were interested in evaluating the AKAP12 gene and protein expression in LV extracts from patients with cardiac injury. Remarkably, AKAP12 was significantly upregulated in the failing hearts compared with nonfailing hearts. One limitation of our study was the low number of samples; therefore, we were not able to correlate confounding diseases, sex, and drug therapies with AKAP12 expression. Further studies with a larger cohort would address this limitation. Nonetheless, our data is in line with several transcriptomic studies that have been conducted on LV extracts from patients with end-stage HF, which have been discussed in detail by Flores et al.[25] Current therapeutics have many off-target pharmacological effects, which could be reduced by subcellular drug delivery. Hence, AKAPs that form microdomains within the cells have been suggested as targets for precision pharmacology.[51] Thus, AKAP12 may be a good candidate for ameliorating HF.

ARTICLE INFORMATION

Received September 8, 2023; revision received February 22, 2024; accepted March 7, 2024.

Affiliations

Department of Pharmacological and Pharmaceutical Sciences, College of Pharmacy (H.Q., M.R., Y.X., A.R.-A., H.Y.A., B.K.M.) and Department of Biology and Biochemistry (M.D.S.), University of Houston, TX. Cardiovascular Research Institute, Departments of Integrative Physiology, Medicine, Neuroscience, Pediatrics, and Center for Space Medicine, Baylor College of Medicine, Houston, TX (S.K.L., X.H.T.W.).

Sources of Funding

This research was supported by the National Heart, Lung, and Blood Institute of the National Institutes of Health under award numbers R15 HL141963 (B.K. McConnell), R01-HL147108, R01-HL153350, and R01-HL089598 (X.H.T. Wehrens), American Heart Association under award number 18AIREA 33960175 (B.K. McConnell) and 23IPA1046060 (B.K. McConnell), and a grant from the Robert J. Kleberg, Jr, and Helen C. Kleberg Foundation (B.K. McConnell). The funders had no role in the preparation of the article or the decision to publish this article.

Disclosures

H. Qasim was employed by IonOptix LLC following the initial article submission. H. Qasim, M. Rajaei, Y. Xu, and B.K. McConnell have a Provisional Patent Application (no. 63/621 310; Modulation of AKAP12 Signalosome; UH Technology Disclosure ID no. 2024-023). The other authors report no conflicts.

Supplemental Material

Expanded Materials and Methods
Figures S1–S8
Videos S1–S4 (related to Figure 3) and Videos S5 and S6 (related to Figure 7)
Tables S1–S6
Data Sets D1 (related to Figure 7) D2 and D3 (related to supplemental Figure 8)
References 52–56
Major Resources Table
Uncut Gel Blots

REFERENCES

1. Madamanchi A. Beta-adrenergic receptor signaling in cardiac function and heart failure. *Mcgill J Med*. 2007;10:99–104. doi: 10.26443/mjm.v10i2.458
2. Tilley DG. G protein-dependent and g protein-independent signaling pathways and their impact on cardiac function. *Circ Res*. 2011;109:217–230. doi: 10.1161/CIRCRESAHA.110.231225
3. Wang J, Gareri C, Rockman HA. G-protein–coupled receptors in heart disease. *Circ Res*. 2018;123:716–735. doi: 10.1161/CIRCRESAHA.118.311403
4. Sadek MS, Cachorro E, El-Armouche A, Kämmerer S. Therapeutic implications for pde2 and cgmp/camp mediated crosstalk in cardiovascular diseases. *Int J Mol Sci*. 2020;21:7462. doi: 10.3390/ijms21207462
5. Colombe A-S, Pidoux G. Cardiac camp-pka signaling compartmentalization in myocardial infarction. *Cells*. 2021;10:922. doi: 10.3390/cells10040922
6. Langeberg LK, Scott JD. A-kinase-anchoring proteins. *J Cell Sci*. 2005;118:3217–3220. doi: 10.1242/jcs.02416
7. Qasim H, McConnell BK. Akap12 signaling complex: Impacts of compartmentalizing camp-dependent signaling pathways in the heart and various signaling systems. *J Am Heart Assoc*. 2020;9:e016615. doi: 10.1161/JAHA.120.016615
8. Tao J, Malbon CC. G-protein-coupled receptor-associated a-kinase anchoring proteins akap5 and akap12: Differential signaling to mapk and gpcr recycling. *J Mol Signal*. 2008;3:19–19. doi: 10.1186/1750-2187-3-19
9. Nichols CB, Rossow CF, Navedo MF, Westenbroek RE, Catterall WA, Santana LF, McKnight GS. Sympathetic stimulation of adult cardiomyocytes requires association of akap5 with a subpopulation of l-type calcium channels. *Circ Res*. 2010;107:747–756. doi: 10.1161/CIRCRESAHA.109.216127
10. Willoughby D, Wong W, Schaack J, Scott JD, Cooper DM. An anchored pka and pde4 complex regulates subplasmalemmal camp dynamics. *EMBO J*. 2006;25:2051–2061. doi: 10.1038/sj.emboj.7601113
11. Fan G, Shumay E, Wang H, Malbon CC (2001) The scaffold protein gravin (cAMP-dependent protein kinase-anchoring protein 250) binds the beta 2-adrenergic receptor via the receptor cytoplasmic Arg-329 to Leu-413 domain and provides a mobile scaffold during desensitization. *J Biol Chem*. 2001;276: 24005–24014. doi: 10.1074/jbc.M011199200
12. Gelman IH. Suppression of tumor and metastasis progression through the scaffolding functions of ssecks/gravin/akap12. *Cancer Metastasis Rev*. 2012;31:493–500. doi: 10.1007/s10555-012-9360-1
13. Havekes R, Canton DA, Park AJ, Huang T, Nie T, Day JP, Guercio LA, Grimes Q, Luczak V, Gelman IH, et al. Gravin orchestrates protein kinase a and beta2-adrenergic receptor signaling critical for synaptic plasticity and memory. *J Neurosci*. 2012;32:18137–18149. doi: 10.1523/JNEUROSCI.3612-12.2012
14. Johnstone TB, Smith KH, Koziol-White CJ, Li F, Kazarian AG, Corpuz ML, Shumyatcher M, Ehlert FJ, Himes BE, Panettieri RA, et al. Pde8 is expressed in human airway smooth muscle and selectively regulates camp signaling by β(2)-adrenergic receptors and adenylyl cyclase 6. *Am J Respir Cell Mol Biol*. 2018;58:530–541. doi: 10.1165/rcmb.2017-0294OC
15. Bagchi RA, Robinson EL, Hu T, Cao J, Hong JY, Tharp CA, Qasim H, Gavin KM, Pires da Silva J, Major JL, et al. Reversible lysine fatty acylation of an anchoring protein mediates adipocyte adrenergic signaling. *Proc Natl Acad Sci USA*. 2022;119:e2119678119. doi: 10.1073/pnas.2119678119
16. Patrucco E, Albergine MS, Santana LF, Beavo JA. Phosphodiesterase 8a (pde8a) regulates excitation-contraction coupling in ventricular myocytes. *J Mol Cell Cardiol*. 2010;49:330–333. doi: 10.1016/j.yjmcc.2010.03.016
17. Leroy J, Vandecasteele G, Fischmeister R. Cyclic amp signaling in cardiac myocytes. *Curr Opin Physiol*. 2018;1:161–171. doi: 10.1016/j.cophys.2017.11.004
18. Boularan C, Gales C. Cardiac camp: production, hydrolysis, modulation and detection. *Front Pharmacol*. 2015;6:203–203. doi: 10.3389/fphar.2015.00203
19. Movsesian MA. Altered camp-mediated signaling and its role in the pathogenesis of dilated cardiomyopathy. *Cardiovasc Res*. 2004;62:450–459. doi: 10.1016/j.cardiores.2004.01.035
20. Zaccolo M. Camp signal transduction in the heart: understanding spatial control for the development of novel therapeutic strategies. *Br J Pharmacol*. 2009;158:50–60. doi: 10.1111/j.1476-5381.2009.00185.x
21. Eisner DA, Caldwell JL, Kistamás K, Trafford AW. Calcium and excitation-contraction coupling in the heart. *Circ Res*. 2017;121:181–195. doi: 10.1161/CIRCRESAHA.117.310230
22. Werhahn SM, Kreusser JS, Hagenmüller M, Beckendorf J, Diemert N, Hoffmann S, Schultz J-H, Backs J, Dewenter M. Adaptive versus maladaptive cardiac remodelling in response to sustained β-adrenergic stimulation in a new 'iso on/off model'. *PLoS One*. 2021;16:e0248933. doi: 10.1371/journal.pone.0248933
23. Chang SC, Ren S, Rau CD, Wang JJ. Isoproterenol-induced heart failure mouse model using osmotic pump implantation. *Methods Mol Biol*. 2018;1816:207–220. doi: 10.1007/978-1-4939-8597-5_16
24. Pan Y, Gao J, Gu R, Song W, Li H, Wang J, Gu Y, Chen H, Zhang H. Effect of injection of different doses of isoproterenol on the hearts of mice. *BMC Cardiovasc Disord*. 2022;22:409. doi: 10.1186/s12872-022-02852-x
25. Flores ROR, Lanzer JD, Holland CH, Leuschner F, Most P, Schultz JH, Levinson RT, Saez-Rodriguez J. Consensus transcriptional landscape of human end-stage heart failure. *J Am Heart Assoc*. 2021;10:e019667. doi: 10.1161/JAHA.120.019667
26. Zoccarato A, Surdo NC, Aronsen JM, Fields LA, Mancuso L, Dodoni G, Stangherlin A, Livie C, Jiang H, Sin YY, et al. Cardiac hypertrophy is inhibited by a local pool of camp regulated by phosphodiesterase 2. *Circ Res*. 2015;117:707–719. doi: 10.1161/CIRCRESAHA.114.305892
27. Karam S, Margaria JP, Bourcier A, Mika D, Varin A, Bedioune I, et al. Cardiac overexpression of pde4b blunts β-adrenergic response and maladaptive remodeling in heart failure. *Circulation*. 2020;142:161–174. doi: 10.1161/CIRCULATIONAHA.119.042573
28. Xiang YK. Compartmentalization of beta-adrenergic signals in cardiomyocytes. *Circ Res*. 2011;109:231–244. doi: 10.1161/CIRCRESAHA.110.231340
29. Steinberg SF. The molecular basis for distinct β-adrenergic receptor subtype actions in cardiomyocytes. *Circ Res*. 1999;85:1101–1111. doi: 10.1161/01.res.85.11.1101
30. Rudokas MW, Post JP, Sataray-Rodriguez A, Sherpa RT, Moshal KS, Agarwal SR, Harvey RD. Compartmentation of β2-adrenoceptor stimulated camp responses by phosphodiesterase types 2 and 3 in cardiac ventricular myocytes. *Br J Pharmacol*. 2021;178:1574–1587. doi: 10.1111/bph.15382
31. Rich TC, Fagan KA, Tse TE, Schaack J, Cooper DM, Karpen JW. A uniform extracellular stimulus triggers distinct camp signals in different compartments of a simple cell. *Proc Natl Acad Sci USA*. 2001;98:13049–13054. doi: 10.1073/pnas.221381398
32. Houslay MD, Baillie GS, Maurice DH. Camp-specific phosphodiesterase-4 enzymes in the cardiovascular system: a molecular toolbox for generating compartmentalized camp signaling. *Circ Res*. 2007;100:950–966. doi: 10.1161/01.RES.0000261934.56938.38
33. Zaccolo M, Pozzan T. Discrete microdomains with high concentration of camp in stimulated rat neonatal cardiac myocytes. *Science*. 2002;295:1711–1715. doi: 10.1126/science.1069982
34. Diviani D, Osman H, Delaunay M, Kaiser S. The role of a-kinase anchoring proteins in cardiac oxidative stress. *Biochem Soc Trans*. 2019;47:1341–1353. doi: 10.1042/BST20190228
35. Wong W, Goehring AS, Kapiloff MS, Langeberg LK, Scott JD. Makap compartmentalizes oxygen-dependent control of hif-1α. *Sci Signaling*. 2008;1:ra18–ra18. doi: 10.1126/scisignal.2000026
36. Lygren B, Carlson CR, Santamaria K, Lissandron V, McSorley T, Litzenberg J, Lorenz D, Wiesner B, Rosenthal W, Zaccolo M, et al. Akap complex regulates ca2+ re-uptake into heart sarcoplasmic reticulum. *EMBO Rep*. 2007;8:1061–1067. doi: 10.1038/sj.embor.7401081
37. Marx SO, Kurokawa J, Reiken S, Motoike H, D'Armiento J, Marks AR, Kass RS. Requirement of a macromolecular signaling complex for β adrenergic receptor modulation of the kcnq1-kcne1 potassium channel. *Science*. 2002;295:496–499. doi: 10.1126/science.1066843
38. Tingley WG, Pawlikowska L, Zaroff JG, Kim T, Nguyen T, Young SG, Vranizan K, Kwok P-Y, Whooley MA, Conklin BR. Gene-trapped mouse embryonic stem cell-derived cardiac myocytes and human genetics implicate akap10 in heart rhythm regulation. *Proc Natl Acad Sci U S A*. 2007;104:8461–8466. doi: 10.1073/pnas.0610393104
39. Guillory AN, Yin X, Wijaya CS, Diaz Diaz AC, Rababa'h A, Singh S, Atrooz F, Sadayappan S, McConnell BK. Enhanced cardiac function in gravin mutant mice involves alterations in the beta- adrenergic receptor signaling cascade. *PLoS One*. 2013;8:e74784. doi: 10.1371/journal.pone.0074784

40. Li Z, Singh S, Suryavanshi SV, Ding W, Shen X, Wijaya CS, Gao WD, McConnell BK. Force development and intracellular ca(2+) in intact cardiac muscles from gravin mutant mice. *Eur J Pharmacol*. 2017;807:117–126. doi: 10.1016/j.ejphar.2017.04.020
41. Fan Q, Yin X, Rababa'h A, Diaz Diaz A, Wijaya CS, Singh S, Suryavanshi SV, Vo HH, Saeed M, Zhang Y, et al. Absence of gravin-mediated signaling inhibits development of high-fat diet-induced hyperlipidemia and atherosclerosis. *Am J Physiol Heart Circ Physiol*. 2019;317:H793–H810. doi: 10.1152/ajpheart.00215.2019
42. Johnson KR, Nicodemus-Johnson J, Spindler MJ, Carnegie GK. Genome-wide gene expression analysis shows akap13-mediated pkd1 signaling regulates the transcriptional response to cardiac hypertrophy. *PLoS One*. 2015;10:e0132474. doi: 10.1371/journal.pone.0132474
43. Garcia-Pelagio KP, Chen L, Joca HC, Ward C, Jonathan Lederer W, Bloch RJ. Absence of synemin in mice causes structural and functional abnormalities in heart. *J Mol Cell Cardiol*. 2018;114:354–363. doi: 10.1016/j.yjmcc.2017.12.005
44. Azevedo MF, Faucz FR, Bimpaki E, Horvath A, Levy I, de Alexandre RB, Ahmad F, Manganiello V, Stratakis CA. Clinical and molecular genetics of the phosphodiesterases (PDEs). *Endocr Rev*. 2014;35:195-233. doi: 10.1210/er.2013-1053
45. Krishnamurthy S, Moorthy BS, Xin Xiang L, Xin Shan L, Bharatham K, Tulsian NK, Mihalek I, Anand GS. Active site coupling in pde:Pka complexes promotes resetting of mammalian camp signaling. *Biophys J*. 2014;107:1426–1440. doi: 10.1016/j.bpj.2014.07.050
46. Fields LA, Koschinski A, Zaccolo M. Sustained exposure to catecholamines affects camp/pka compartmentalised signalling in adult rat ventricular myocytes. *Cell Signal*. 2016;28:725–732. doi: 10.1016/j.cellsig.2015.10.003
47. Woo AYH, Xiao R-ping. B-adrenergic receptor subtype signaling in heart: from bench to bedside. *Acta Pharmacol Sin*. 2012;33:335–341. doi: 10.1038/aps.2011.201
48. Fajardo G, Zhao M, Urashima T, Farahani S, Hu D-Q, Reddy S, Bernstein D. Deletion of the β2-adrenergic receptor prevents the development of cardiomyopathy in mice. *J Mol Cell Cardiol*. 2013;63:155–164. doi: 10.1016/j.yjmcc.2013.07.016
49. Grammatika Pavlidou N, Dobrev S, Beneke K, Reinhardt F, Pecha S, Jacquet E, Abu-Taha IH, Schmidt C, Voigt N, Kamler M, et al. Phosphodiesterase 8 governs camp/pka-dependent reduction of l-type calcium current in human atrial fibrillation: a novel arrhythmogenic mechanism. *Eur Heart J*. 2023;44:2483–2494. doi: 10.1093/eurheartj/ehad086
50. Rigatti M, Le AV, Gerber C, Moraru II, Dodge-Kafka KL. Phosphorylation state-dependent interaction between akap7δ/γ and phospholamban increases phospholamban phosphorylation. *Cell Signal*. 2015;27:1807–1815.
51. Omar MH, Scott JD. Akap signaling islands: venues for precision pharmacology. *Trends Pharmacol Sci*. 2020;41:933–946. doi: 10.1016/j.tips.2020.09.007
52. Gulick J, Subramaniam A, Neumann J, Robbins J. Isolation and characterization of the mouse cardiac myosin heavy chain genes. *J Biol Chem*. 1991;266:9180–9185. doi: 10.1016/S0021-9258(18)31568-0
53. Gibson DG, Young L, Chuang RY, Venter JC, Hutchison CA 3rd, Smith HO. Enzymatic assembly of DNA molecules up to several hundred kilobases. *Nat Methods*. 2009;6:343–345. doi: 10.1038/nmeth.1318
54. Lindsey ML, Kassiri Z, Virag JAI, de Castro Bras LE, Scherrer-Crosbie M. Guidelines for measuring cardiac physiology in mice. *Am J Physiol Heart Circ Physiol*. 2018;314:H733–H752. doi: 10.1152/ajpheart.00339.2017
55. Ackers-Johnson M, Li PY, Holmes AP, O'Brien S-M, Pavlovic D, Foo RS. A simplified, langendorff-free method for concomitant isolation of viable cardiac myocytes and nonmyocytes from the adult mouse heart. *Circ Res*. 2016;119:909–920. doi: 10.1161/CIRCRESAHA.116.309202
56. Davidson MM, Nesti C, Palenzuela L, Walker WF, Hernandez E, Protas L, Hirano M, Isaac ND. Novel cell lines derived from adult human ventricular cardiomyocytes. *J Mol Cell Cardiol*. 2005;39:133–147. doi: 10.1016/j.yjmcc.2005.03.003